ORIGINAL ARTICLE

Fast UV detection by Cu-doped ZnO nanorod arrays chemically deposited on PET substrate

Reza Shabannia

Department of Physics, College of Science, Babol Noshirvani University of Technology, Babol, Iran

Abstract
Well-aligned Cu-doped ZnO nanorods were successfully synthesized on polyethylene terephthalate (PET) substrate using chemical bath deposition method. The structural and optical properties of Cu-doped ZnO nanorods were investigated using X-ray diffraction (XRD), field-emission scanning electron microscopy (FESEM), energy dispersive X-ray spectroscopy (EDX) and photoluminescence (PL) spectroscopy. A metal-semiconductor-metal (MSM) UV photodetector was successfully fabricated using high-quality Cu-doped ZnO nanorods. The dark current and photocurrent of the MSM photodetector based on Cu doped ZnO nanorods were 20.5 μA and 2.22 mA at bias voltage of 5 V, respectively. Under bias voltage of 5 V, the responsivity of the UV photodetector was *3.69 A/W*. The calculated photosensitivity of the UV photodetector was 107.4 at bias voltage of 5 V. The fast response time (191 ms) and recovery time (261 ms) of the fabricated UV photodetectors were achieved in UV turn-on/off switching measurements.

Keywords: *Chemical Bath Deposition; Crystal Structure; Cu-doped ZnO Nanorods; Polyethylene Terephthalate; UV Photodetector.*

INTRODUCTION

Recently, zinc oxide (ZnO) nanorods have been received considerable attention from many researchers because of its high thermal stability, high conductivity and transparency in the visible wavelength region. These ZnO nanorods can be applied in optoelectronic devices such as display panels, light emitting diode, solar cells, chemical sensor, photovoltaic device, and ultraviolet (UV) photodetectors [1-4]. Due to the wide range of chemical and environmental detecting applications, the UV detectors are applicable for detecting UV radiation with different wavelengths. Compared with the devices based on bulk ZnO and different nanostructures, the aligned ZnO nanorod arrays are able to provide faster response and higher sensitivity due to their much higher surface area to volume ratio [5-7]. In the recent years, several reports have been demonstrated that the conductivity of ZnO nanostructures can be improved by doping with various dopants

and thermal treatment [8-13]. Among these different doping elements, copper is so important because of its prominent luminescence activator which can modify the luminescence of ZnO nanostructures by creating localized impurity levels [14]. Moreover, the physical and chemical properties of Cu is similar to those of Zn, and it can affect the microstructure and optical properties of ZnO [15]. Among different ZnO structures with various dopants , Cu doped ZnO nanostructures are particularly attractive because of their transparency, high conductivity and relatively low cost of fabrication [16-17]. Despite the importance of Cu doped ZnO nanorods, until now only few works have been reported on the synthesis of these nanostructures through solution growth methods on various substrates [18-19]. In recent years, flexible polymer substrates are popular for fabrication of portable and low-cost electronic devices. One of the interesting flexible substrates is polyethylene terephthalate (PET) which has good

* Corresponding Author Email: *rezash56rami@gmail.com*

flexibility, high transparency, large surface area, low cost, and availability [20-23]. Farhat *et al.* [23] have reported an ultraviolet photodetector based on vertically aligned ZnO nanorods, which were grown on Teflon substrate by a wet chemical bath deposition method. Manekkathodi *et al.* [20] have fabricated the photodetector with high sensitive properties based on aligned ZnO nanorods on paper substrate by using low temperature chemical solution. To the best of my knowledge, there is no report on UV photodetectors based on Cu doped ZnO nanorod arrays grown on a flexible PET substrate using chemical bath deposition (CBD) method. In this research, a fast, low-cost and sensitive UV detector is presented based on vertically well-aligned Cu doped ZnO nanorods grown on a flexible PET substrate using CBD technique.

MATERIALS AND METHODS

The flexible PET wafer was utilized as a substrate for growing Cu-doped ZnO nanorods by CBD method. PET substrates were ultrasonically cleaned in a glass beaker containing isopropyl alcohol solution at 50 °C for 20 min. The ZnO seed layer was deposited on the prepared PET substrates by a radio-frequency magnetron sputtering system for the growth of the vertically aligned ZnO nanorods. A 100 nm ZnO seed layer was fabricated on PET substrate. The chemical solution for deposition of Cu-doped ZnO nanostructures (with nominal fraction values of 2 at.%) were prepared by dissolving zinc nitrate hexahydrate ($Zn(NO_3)_2 \cdot 6H_2O$, 0.05 M), Copper sulfate pentahydrate ($CuSO_4 \cdot 5H_2O$, 0 and 0.001 M), and hexamethylenetetramine ($C_6H_{12}N_4$, 0.05 M) in deionized (DI) water. The solution was then stirred at 80 °C for three minutes. The prepared PET substrates were vertically dipped inside the beaker. For growth of the ZnO nanorods, the beaker was transferred inside an oven for 5 h at the temperature was fixed at 90 °C.

The structure and orientation of the undoped ZnO and Cu-doped ZnO nanorods were determined by X-ray diffraction (PANalytical X'Pert PRO MRD PW3040). Surface morphology and elemental analysis of the synthesized materials were examined by field emission scanning electron microscopy and energy dispersive X-ray spectroscopy (model FEI/ Nova NanoSEM 450). Photoluminescence (PL) spectroscopy (Jobin Yvon HR 800 UV, Edison, NJ, USA) was used to characterize the optical properties of the ZnO nanorods at room temperature. Current–voltage characteristics of ZnO nanorods were performed with increasing step of applied voltage 0.01 V within the voltage range from -5.0 V to +5.0 V by using a computer-controlled integrated source meter (Keithley 2400) at room temperature. A 365 nm UV lamp with an illumination intensity of approximately 3 mW/cm^2 was employed as an excitation source during the photoelectric measurements.

RESULTS AND DISCUSSION
Characterization of the ZnO nanorods

Fig. 1 demonstrates a typical XRD pattern of Cu-doped ZnO nanorods grown on PET substrate. From the Fig. 1 it is seen that the growth of nanorod is along (1 0 0) and (0 0 2) plane and matched the wurtzite hexagonal phase of bulk ZnO (ICSD 01-080-0074). A (002) peak in the XRD
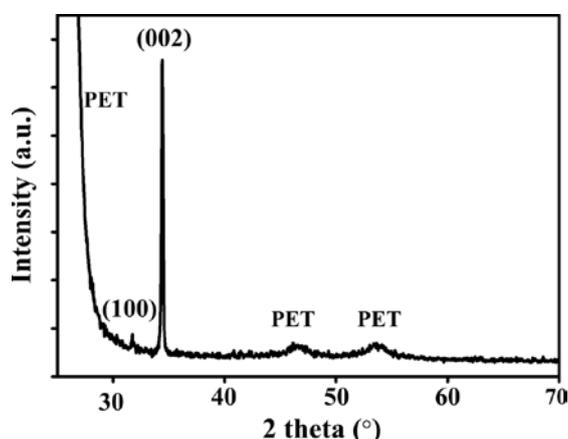
Fig. 1. XRD pattern of the Cu-doped ZnO nanorods grown on PET substrate.

pattern indicates that the Cu-doped ZnO nanorods are oriented along the c-axis. The calculated grain size and strain of Cu-doped ZnO nanorods were 73.9 nm and -0.1783%, respectively. The low compressive strain, high intensity and the narrow width of the (002) diffraction peak exhibited that the Cu-doped ZnO nanorods with improved crystal quality were grown vertically on the PET substrate.

Fig. 2 shows the FESEM image of the surface morphology of the aligned Cu-doped ZnO nanorods synthesized on PET substrate. Fig. 2 demonstrates that the diameter of the Cu-doped ZnO nanorods grown on PET substrate changed from 25 nm to 99 nm. The most of diameter of Cu-doped ZnO nanorods are less than 50 nm. The well-aligned Cu-doped ZnO nanorods with high density are interesting nanostructures for sensing applications in dye sensitized solar cells and photodetection device [24].

Fig. 3 illustrates the PL spectrum of the Cu-doped ZnO nanorods grown on PET substrate in the wavelength range of 350-1000 nm using He-Cd laser with the excitation wavelength 325nm. The Cu-doped ZnO nanorod arrays have a sharp and high -intensity UV emission peak centered at 381.5 nm and a broad and low-intensity visible emission peak centered at 534 nm. The UV emission is due to the recombination of free excitons through an exciton–exciton collision process [25], whereas the visible emission is due to the recombination of photogenerated holes with singly ionized charge states in intrinsic defects, such as Zn interstitials, impurities, and oxygen vacancies [26]. The higher UV emission peak compared with the weak spectral bands in the visible region in PL spectra showed that the good structure of Cu-doped ZnO nanorods with few structural and surface defects.

The chemical composition of the synthesized materials was analyzed using EDX analysis. A typical EDX spectrum of Cu doped ZnO nanorods grown on PET substrate is demonstrated in Fig. 4, which confirmed the presence of copper in ZnO
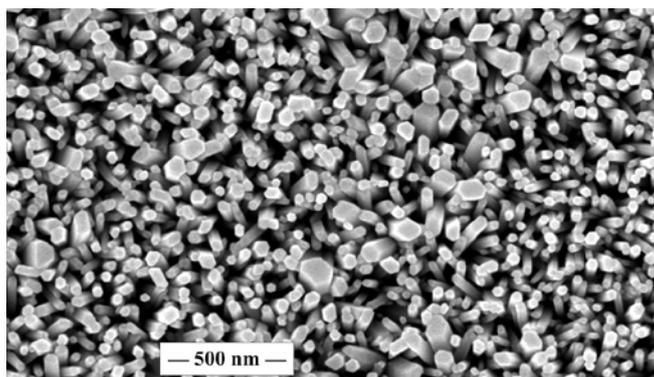
Fig. 2. Surface FESEM image of Cu-doped ZnO nanorods grow on PET substrate.
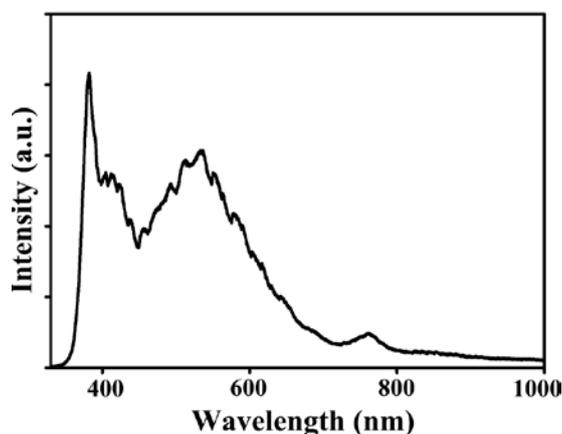
Fig. 3. PL spectrum of the Cu-doped ZnO nanorods grown on PET substrate.

nanorods. It was found that the real Cu/Zn molar ratio was lower than nominal fraction value in the deposition solutions.

Characteristics of the ZnO nanorod MSM UV photodetector

To examine the performance of Cu doped ZnO nanorods, the UV photodetector device were fabricated with Cu doped ZnO nanorod arrays grown on PET substrate. A Pt layer was deposited on the top of the Cu doped ZnO nanorod arrays as illustrated in the inset of Fig. 5. The current–voltage curve (I–V) of the UV photodetector device in the dark and under UV (365 nm) illumination by changing the bias voltage from −5 V to +5 V at room temperature is shown in Fig. 5.

The high photocurrent achieved for UV photodetector device can be attributed to good crystalline quality of Cu-doped ZnO nanorods, which it can be accredited to the significantly suppressed recombination of photogenerated charge carriers [27]. When the Cu-doped ZnO nanorods based UV photodetector is exposed under UV light, electron-hole pairs are photo-generated ($h\nu \rightarrow e^- + h^+$) and holes are captured by the negative oxygen ions in surface of the ZnO nanorods through surface electron-hole recombination ($h^+ + O_2^-(adsorbed) \rightarrow O_2(gas)$). Consequently, an increase in the free carrier concentration and a decrease in the width of the depletion layer, because of oxygen atoms desorbed from the ZnO nanorod surfaces. Thus, the photogenerated free electrons in the conduction band contribute to increase the conductivity of the photodetector [28-29]. The measured dark current (I_d) and photocurrent (I_{ph}) of the UV photodetector based on Cu doped ZnO nanorods are 20.5 μA and 2.22 MA at 5 V bias
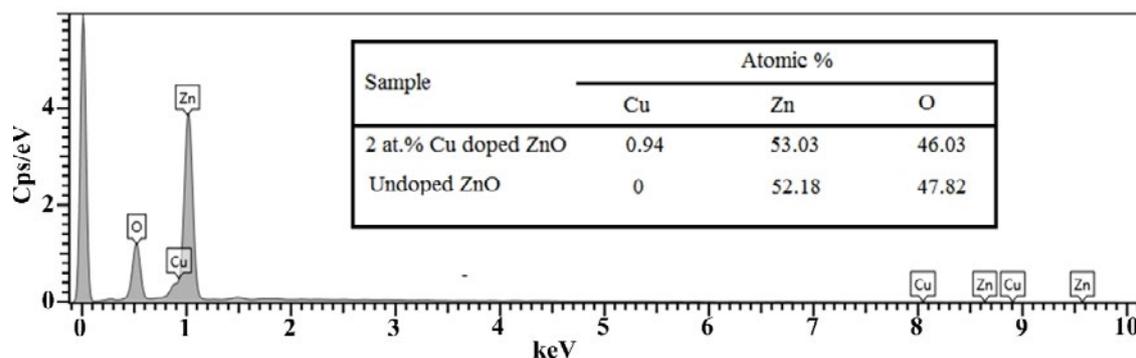
Fig. 4 EDX spectrum of Cu doped ZnO nanorods grown on PET substrate.
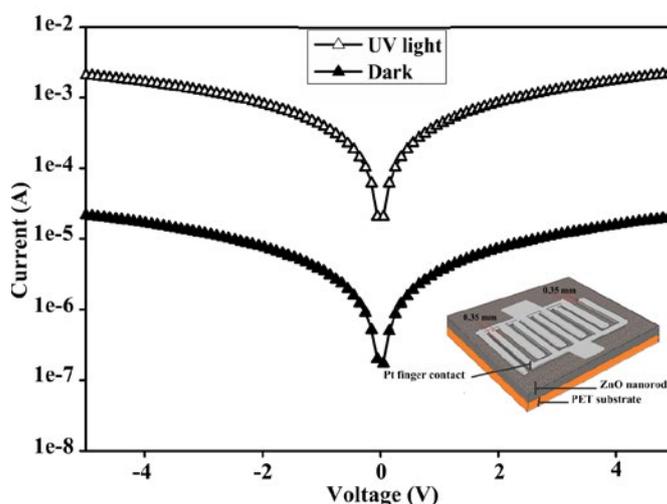
Fig. 5. I–V plot of the Cu doped ZnO nanorods UV photodetector in the dark and under UV (365 nm) illumination. Inset is the schematic diagram of the Pt interdigitated finger shaped contacts on ZnO nanorods for UV detection application.
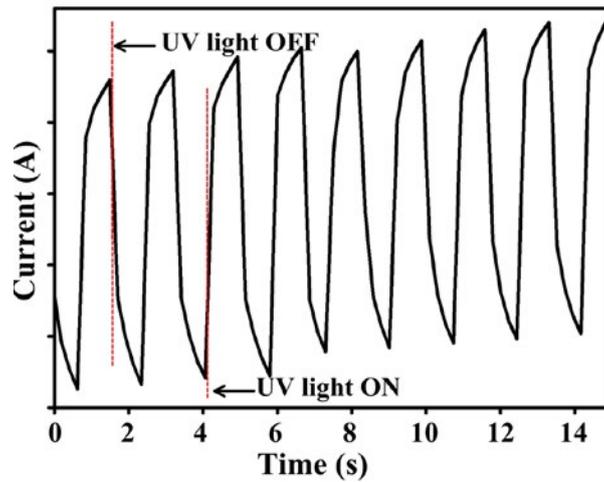
Fig. 6. The photoresponse of Cu-doped ZnO nanorods UV photodetector.

Table 1. Photoelectrical parameters of UV detectors based on ZnO and Cu-doped ZnO nanorods.

Device structure	Bias voltage (V)	Response time (s)	Recovery time (s)	Responsivity (A/W)	Reference
Cu doped ZnO nanorods on PET	5	0.191	0.261	3.692	This work
ZnO nanorods on PET	0.5	100	120	0.222	[32]
ZnO nanorods on Teflon	5	6.7	9.3	2.265	[23]
ZnO nanorods on PEN	3	1.2	1.8	2.856	[31]

voltage, respectively. The responsivity of the Cu doped ZnO nanorods MSM photodetector was obtained using the following relationship [30]:

$$R = \frac{I_{ph}(A)}{E(W/cm^2)A(cm^2)} \tag{1}$$

where I_{ph}, E and A are the photocurrent, intensity of UV light and effective area of the device, respectively. At applied bias voltage of 5 V, the responsivity of the fabricated UV photodetector was *3.69 A/W*.

The photosensitivity of the fabricated UV photodetector was obtained using the following equation [31]:

$$S = \frac{I_{ph} - I_d}{I_d} \tag{2}$$

where I_{ph} and I_d are the photocurrent and dark current, respectively. The photosensitivity of the photodetector was 107.4 at 5 V bias voltage. Cu dopants often act as a deep acceptor in ZnO nanorods and reduce the n type carrier concentration by trapping electron. Therefore, this results lead to the lower dark current and produces an opportunity to improve photoresponse sensitivity.

The dynamic response time measurement was used to study the optical response through exposing the device to a UV light illumination to test the reversibility of the fabricated UV photodetector. Fig. 6 displays the obtained photoresponse of the UV photodetector as a function of time by switching on and off UV light (365 nm) at 5 V bias voltage. As shown in Fig. 6, the measured photocurrent of device rapidly increased by switching on the UV light and then decreased under dark condition. The response time is the time needed to reach the photocurrent to 80 % of its saturation value, while the recovery time is the time needed to drop the photocurrent to 20 % of its saturation value. The values of the obtained response time and recovery time of the MSM UV photodetector were 0.191 s and 0.261 s, respectively. The fast response time can be attributed to the reduced carrier transit times in low-diameter Cu doped ZnO nanorods, While the fast recovery time can be related to the rapid electron–hole pair recombination process by switching off the UV light [31]. A comparison between the current research and previous studies of UV detectors based on ZnO and Cu-doped ZnO nanorods is also shown in Table 1.

CONCLUSIONS

The Cu-doped ZnO nanorod arrays have been successfully fabricated on flexible PET substrate by chemical bath deposition method. The structural, optical and their UV detection properties of Cu-doped ZnO nanorods were investigated. At applied bias voltage of 5 V, the responsivity of the fabricated UV photodetector was *3.69 A/W*. The photosensitivity of the fabricated UV photodetector was 107.4 at 5 V bias voltage. The values of the obtained response time and recovery time of the MSM UV photodetector were 0.191 s and 0.261 s, respectively.

ACKNOWLEDGMENT

CONFLICT OF INTEREST

The authors declare that there are no conflicts of interest regarding the publication of this manuscript.

REFERENCES

[1] Ohta H., Hosono H., (2004), Transparent oxide optoelectronics. *Mater. Today.* 7: 42-51.

[2] Tonooka K., Bando H., Aiura Y., (2003), Photovoltaic effect observed in transparent p–n heterojunctions based on oxide semiconductors. *Thin Solid Films.* 445: 327-331.

[3] Zhai T., Li L., Wang X., Fang X., Bando Y., Golberg D., (2010), Recent developments in one-dimensional inorganic nanostructures for photodetectors. *Adv. Funct. Mater.* 20: 4233-4248.

[4] Hassan J., Mahdi M., Kasim S., Ahmed N. M., Hassan H. A., Hassan Z., (2013), Fast UV detection and hydrogen sensing by ZnO nanorod arrays grown on a flexible Kapton tape. *Mater. Sci. Poland.* 31: 180-185.

[5] Rejani P., Radhakrishnan A., Beena B., (2014), Structural, optical and dielectric studies in ZnO nanorods by microwave assisted method. *Int. J. Nano Dimens.* 5: 497-503.

[6] Janitabar Darzi S., Mahjoub A., Bayat A., (2015), Sulfur modified ZnO nanorod as a high performance photocatalyst for degradation of Congoredazo dye. *Int. J. Nano Dimens.* 6: 425-431.

[7] Aula S., Lakkireddy S., Kapley A., Adimadhyam V. N., Sharma R., Uppin S., Jamil K., (2018), Route of administration induced in vivo effects and toxicity responses of Zinc Oxide nanorods at molecular and genetic levels. *Int. J. Nano Dimens.* 9: 158-169.

[8] Shabannia R., (2016), Effect of annealing temperature on the structural, optical and electrical properties of ZnO thin films grown chemically on PS substrate. *J. Mater. Sci. Mater. Electro.* 27: 6413-6418.

[9] Lee J.-H., Park B.-O., (2003), Transparent conducting ZnO: Al, In and Sn thin films deposited by the sol–gel method. *Thin Solid Films.* 426: 94-99.

[10] Ohyama M., Kozuka H., Yoko T., (1998), Sol-gel preparation of transparent and conductive aluminum-doped zinc oxide films with highly preferential crystal orientation. *J. Am. Ceram. Soc.* 81: 1622-1632.

[11] Yamamoto Y., Saito K., Takahashi K., Konagai M., (2001), Preparation of boron-doped ZnO thin films by photo-atomic layer deposition. *Sol. Energy Mater. Sol. Cells.* 65: 125-132.

[12] Hsu C.-H., Chen D.-H., (2010), Synthesis and conductivity enhancement of Al-doped ZnO nanorod array thin films. *Nanotechnol.* 21: 285603.

[13] Shewale P., Yu Y., (2016), Structural, surface morphological and UV photodetection properties of pulsed laser deposited Mg-doped ZnO nanorods: effect of growth time. *J. Alloys Compd.* 654: 79-86.

[14] Tao Y., Ma S., Chen H., Meng J., Hou L., Jia Y., Shang X., (2011), Effect of the oxygen partial pressure on the microstructure and optical properties of ZnO : Cu films. *Vacuum.* 85: 744-748.

[15] Zhang Z., Yi J. B., Ding J., Wong L. M., Seng H. L., Wang S. J., Tao J. G., Li G. P., Xing G. Z., Sum T. C., (2008), Cu-doped ZnO nanoneedles and nanonails: Morphological evolution and physical properties. *J. Phys. Chem. C.* 112: 9579-9585.

[16] Lv J., Liu C., Gong W., Zi Z., Chen X., Huang K., Liu F., Wang T., He G., Song X., (2012), Facile synthesis of Zn 1− x Cu x O nanorods with a very broad visible band. *Electro. Mater. Lett.* 8: 477-480.

[17] Bhuyan T., Khanuja M., Sharma R., Patel S., Reddy M., Anand S., Varma A., (2015), A comparative study of pure and copper (Cu)-doped ZnO nanorods for antibacterial and photocatalytic applications with their mechanism of action. *J. Nanopart. Res.* 17: 288-293.

[18] Babikier M., Wang D., Wang J., Li Q., Sun J., Yan Y., Yu Q., Jiao S., (2014), Cu-doped ZnO nanorod arrays: the effects of copper precursor and concentration. *Nanoscale Res. Lett.* 9: 199-206.

[19] Polat İ., Yılmaz S., Altın İ., Bacaksız E., Sökmen M. (2014), The influence of Cu-doping on structural, optical and photocatalytic properties of ZnO nanorods. *Mater. Chem. Phys.* 148: 528-532.

[20] Manekkathodi A., Lu M. Y., Wang C. W., Chen L. J., (2010), Direct growth of aligned zinc oxide nanorods on paper substrates for low-cost flexible electronics. *Adv. Mater.* 22: 4059-4063.

[21] Jin Y., Wang J., Sun B., Blakesley J. C., Greenham N. C., (2008), Solution-processed ultraviolet photodetectors based on colloidal ZnO nanoparticles. *Nano lett.* 8: 1649-1653.

[22] Lee C. Y., Li S. Y., Lin P., Tseng T. Y., (2005), ZnO nanowires hydrothermally grown on PET polymer substrates and their characteristics. *J. Nanosci. Nanotechnol.* 5: 1088-1094.

[23] Farhat O., Halim M., Abdullah M., Ali M., Ahmed N. M., Allam N. K., (2015), Growth of vertically aligned ZnO nanorods on Teflon as a novel substrate for low-power flexible light sensors. *Appl. Phys. A.* 119: 1197-1201.

[24] Lockett A. M., Thomas P. J., O'Brien P., (2012), Influence of seeding layers on the morphology, density, and critical dimensions of ZnO nanostructures grown by chemical bath deposition. *J. Phys. Chem. C.* 116: 8089-8094.

[25] Shabannia R., Hassan H. A., (2013), Growth and characterization of vertically aligned ZnO nanorods grown on porous silicon: Effect of precursor concentration. *Superlatt. Microstruc.* 62: 242-250.

[26] Kenanakis G., Androulidaki M., Koudoumas E., Savvakis C., Katsarakis N., (2007), Photoluminescence of ZnO

nanostructures grown by the aqueous chemical growth technique. *Superlatt. Microstruc.* 42: 473-478.

[27] Inamdar S., Rajpure K., (2014), High-performance metal–semiconductor–metal UV photodetector based on spray deposited ZnO thin films. *J. Alloys Compd.* 595: 55-59.

[28] Shabannia R., Hassan H. A., Mahmodi H., Naderi N., Abd H., (2013), ZnO nanorod ultraviolet photodetector on porous silicon substrate. *Semicond. Sci. Techno.* 28: 115007.

[29] Soci C., Zhang A., Xiang B., Dayeh S. A., Aplin D., Park J., Bao X., Lo Y.-H., Wang D., (2007), ZnO nanowire UV photodetectors with high internal gain. *Nano Let.* 7**:** 1003-1009.

[30] Selman A. M., Hassan Z., (2015), Highly sensitive fast-response UV photodiode fabricated from rutile TiO_2 nanorod array on silicon substrate. *Sens. Actuators A. Phys.* 221: 15-21.

[31] Shabannia R., Hassan H. A., (2014), Characteristics of photoconductive UV photodetector based on ZnO nanorods grown on polyethylene naphthalate substrate by chemical bath deposition method. *Electro. Mater. Lett.* 10: 837-843.

[32] Yao I.-C., Tseng T.-Y., Lin P., (2012), ZnO nanorods grown on polymer substrates as UV photodetectors. *Sens. Actuators A. Phys.* 178: 26-31.